

Long-distance quantum communication with atomic ensembles and linear optics

L.-M. Duan^{1,2*}, M. Lukin³, J. I. Cirac^{1†}, and P. Zoller¹

¹*Institut für Theoretische Physik, Universität Innsbruck, A-6020 Innsbruck, Austria*

²*Laboratory of Quantum Communication and Computation, USTC, Hefei 230026, China*

³*ITAMP, Harvard-Smithsonian Center for Astrophysics, Cambridge, MA 02138*

Quantum communication holds a promise for absolutely secure transmission of secret messages and faithful transfer of unknown quantum states. Photonic channels appear to be very attractive for physical implementation of quantum communication. However, due to losses and decoherence in the channel, the communication fidelity decreases exponentially with the channel length. We describe a scheme that allows to implement robust quantum communication over long lossy channels. The scheme involves laser manipulation of atomic ensembles, beam splitters, and single-photon detectors with moderate efficiencies, and therefore well fits the status of the current experimental technology. We show that the communication efficiency scale polynomially with the channel length thereby facilitating scalability to very long distances.

The goal of quantum communication is to transmit quantum states between distant sites. One the one hand, this has an important potential application for secret transfer of classical messages by means of quantum cryptography [1]. On the other hand, it is also an essential element required for constructing quantum networks. The basic problem of quantum communication is to generate nearly perfect entangled states between distant sites. Such states can be used, for example, to implement secure quantum cryptography using the Ekert protocol [1], and to faithfully transfer quantum states via quantum teleportation [2]. All realistic schemes for quantum communication are presently based on the use of the photonic channels. However, the degree of entanglement generated between two distant sites normally decreases exponentially with the length of the connecting channel due to the optical absorption and other channel noise. To regain a high degree of entanglement purification schemes can be used [3]. However, entanglement purification does not fully solve the long-distance communication problem. Due to the exponential decay of the entanglement in the channel, one needs an exponentially large number of partially entangled states to obtain one highly entangled state, which means that for a sufficiently long distance the task becomes nearly impossible.

To overcome the difficulty associated with the exponential fidelity decay, the concept of quantum repeaters

can be used [4]. In principle, it allows to make the overall communication fidelity very close to the unity, with the communication time growing only polynomially with the transmission distance. In analogy to a fault-tolerant quantum computing [5,6] the quantum repeater proposal is a cascaded entanglement purification protocol for communication systems. The basic idea is to divide the transmission channel into many segments, with the length of each segment comparable to the channel attenuation length. First, one generates entanglement and purifies it for each segment; the purified entanglement is then extended to a longer length by connecting two adjacent segments through entanglement swapping [2,7]. After entanglement swapping, the overall entanglement is decreased, and one has to purify it again. One can continue the rounds of the entanglement swapping and purification until a nearly perfect entangled states are created between two distance sites.

To implement the quantum repeater protocol, one needs to generate entanglement between distant quantum bits (qubits), store them for sufficiently long time and perform local collective operations on several of these qubits. The requirement of quantum memory is essential since all purification protocols are probabilistic. When entanglement purification is performed for each segment of the channel, quantum memory can be used to keep the segment state if the purification succeeds and to repeat the purification for the segments only where the previous attempt fails. This is essentially important for polynomial scaling properties of the communication efficiency since with no available memory we have to require that the purifications for all the segments succeeds at the same time; the probability of such event decreases exponentially with the channel length. The requirement of quantum memory implies that we need to store the local qubits in the atomic internal states instead of the photonic states since it is difficult to store photons for a reasonably long time. With atoms as the local information carriers it seems to be very hard to implement quantum repeaters since normally one needs to achieve the strong coupling between atoms and photons with high-finesse cavities for atomic entanglement generation, purification, and swapping [8,9], which, in spite of the recent significant experimental advances [10–12], remains a very challenging technology.

Here, we propose a very different scheme which realizes quantum repeaters and long-distance quantum communication with surprisingly simple physical setups. The

*Email: luming.duan@uibk.ac.at

†Email: Ignacio.Cirac@uibk.ac.at

scheme is a combination of three significant advances for entanglement generation, connection, and applications, with each of the steps having built-in entanglement purification and resilient to the realistic noise. The scheme for the fault-tolerant entanglement generation originates from the earlier proposals to entangle single atoms through single-photon interference at photodetectors [13,14]. However, the present approach involves collective rather than single particle excitations in atomic ensembles, which allows to significantly simplify the realization and greatly improve the generation efficiency. This is the case due to collectively enhanced coupling to light that has been recently investigated both theoretically [15–19] and experimentally [20,21]. The entanglement connection is achieved through simple linear optical operations, and is inherently robust against the realistic imperfections. Different schemes with linear optics are proposed recently for quantum computation [22] and purification [23]. Finally, the resulting state of ensembles after the entanglement connection finds direct applications in realizing the entanglement-based quantum communication protocols, such as quantum teleportation, cryptography, and Bell inequality detection. In all of these applications the mixed entanglement is purified automatically to the nearly perfect entanglement. As a combination of these three breakthroughs, our scheme circumvents the realistic noise and imperfections and provides a feasible method for long-distance high-fidelity quantum communication. The required overhead in the communication time increases with the distance only polynomially.

Entanglement generation

The basic element of our system is a cloud of N_a identical atoms with the relevant level structure shown in Fig. 1. A pair of metastable lower states $|g\rangle$ and $|s\rangle$ can correspond e.g. to hyperfine or Zeeman sublevels of electronic ground state of alkali atoms. Long lifetimes for relevant coherence have been observed both in a room-temperature dilute atomic gas (e.g. in [19,20]) and in a sample of cold trapped atoms (e.g. in [21]). To facilitate enhanced coupling to light, the atomic medium is preferably optically thick along one direction. This can be easily achieved either by working with a pencil shaped atomic sample [19–21] or by placing the sample in a low-finesse ring cavity [16,24] (see Supplementary information).

All the atoms are initially prepared in the ground state $|g\rangle$. A sample is illuminated by a short, off-resonant laser pulse that induces Raman transitions into the states $|s\rangle$. We are particularly interested in the forward-scattered Stokes light that is co-propagating with the laser. Such scattering events are uniquely correlated with the excitation of the symmetric collective atomic mode S [15–21] given by $S \equiv (1/\sqrt{N_a}) \sum_i |g\rangle_i \langle s|$, where the summation is taken over all the atoms. In particular, an emission of the single Stokes photon in a forward direction results in

the state of atomic ensemble given by $S^\dagger|0_a\rangle$, where the ensemble ground state $|0_a\rangle \equiv \bigotimes_i |g\rangle_i$.

We assume that the light-atom interaction time t_Δ is short so that the mean photon number in the forward-scattered Stokes pulse is much smaller than 1. One can define an effective single-mode bosonic operator a for this Stokes pulse with the corresponding vacuum state denoted by $|0_p\rangle$. The whole state of the atomic collective mode and the forward-scattering Stokes mode can now be written in the following form (see the Supplementary information for the technical details)

$$|\phi\rangle = |0_a\rangle |0_p\rangle + \sqrt{p_c} S^\dagger a^\dagger |0_a\rangle |0_p\rangle + o(p_c), \quad (1)$$

where p_c is the small excitation probability and $o(p_c)$ represents the terms with more excitations whose probabilities are equal or smaller than p_c^2 . Before proceeding we note that a fraction of light is emitted in other directions due to the spontaneous emissions. However whenever N_a is large, the contribution to the population in the symmetric collective mode from the spontaneous emissions is small [15–21]. As a result we have a large signal-to-noise ratio for the processes involving the collective mode, which greatly enhances the efficiency of the present scheme (see Box 1 and the Supplementary information).

We now show how to use this setup to generate entanglement between two distant ensembles L and R using the configuration shown in Fig. 1. Here two laser pulses excited both ensembles simultaneously and the whole system is described by the state $|\phi\rangle_L \otimes |\phi\rangle_R$, where $|\phi\rangle_L$ and $|\phi\rangle_R$ are given by Eq. (1) with all the operators and states distinguished by the subscript L or R. The forward scattered Stokes light from both ensembles is combined at the beam splitter and a photodetector click in either D1 or D2 measures the combined radiation from two samples, $a_+^\dagger a_+$ or $a_-^\dagger a_-$ with $a_\pm = (a_L \pm e^{i\varphi} a_R) / \sqrt{2}$. Here, φ denotes an unknown difference of the phase shifts in the two-side channels. We can also assume that φ has an imaginary part to account for the possible asymmetry of the setup, which will also be corrected automatically in our scheme. But the setup asymmetry can be easily made very small, and for simplicity of expressions we assume φ is real in the following. Conditional on the detector click, we should apply a_+ or a_- to the whole state $|\phi\rangle_L \otimes |\phi\rangle_R$, and the projected state of the ensembles L and R is nearly maximally entangled with the form (neglecting the high-order terms $o(p_c)$)

$$|\Psi_\varphi\rangle_{LR}^\pm = (S_L^\dagger \pm e^{i\varphi} S_R^\dagger) / \sqrt{2} |0_a\rangle_L |0_a\rangle_R. \quad (2)$$

The probability for getting a click is given by p_c for each round, so we need repeat the process about $1/p_c$ times for a successful entanglement preparation, and the average preparation time is given by $T_0 \sim t_\Delta / p_c$. The states $|\Psi_r\rangle_{LR}^+$ and $|\Psi_r\rangle_{LR}^-$ can be easily transformed to each

other by a simple local phase shift. Without loss of generality, we assume in the following that we generate the entangled state $|\Psi_r\rangle_{LR}^+$.

As will be shown below, the presence of the noise modifies the projected state of the ensembles to

$$\rho_{LR}(c_0, \varphi) = \frac{1}{c_0 + 1} \left(c_0 |0_a 0_a\rangle_{LR} \langle 0_a 0_a| + |\Psi_\varphi\rangle_{LR}^+ \langle \Psi_\varphi| \right), \quad (3)$$

where the “vacuum” coefficient c_0 is determined by the dark count rates of the photon detectors. It will be seen below that any state in the form of Eq. (3) will be purified automatically to a maximally entangled state in the entanglement-based communication schemes. We therefore call this state an effective maximally entangled (EME) state with the vacuum coefficient c_0 determining the purification efficiency.

Entanglement connection through swapping

After the successful generation of the entanglement within the attenuation length, we want to extend the quantum communication distance. This is done through entanglement swapping with the configuration shown in Fig. 2. Suppose that we start with two pairs of the entangled ensembles described by the state $\rho_{LI_1} \otimes \rho_{I_2R}$, where ρ_{LI_1} and ρ_{I_2R} are given by Eq. (3). In the ideal case, the setup shown in Fig. 2 measures the quantities corresponding to operators $S_\pm^\dagger S_\pm$ with $S_\pm = (S_{I_1} \pm S_{I_2})/\sqrt{2}$. If the measurement is successful (i.e., one of the detectors registers one photon), we will prepare the ensembles L and R into another EME state. The new φ -parameter is given by $\varphi_1 + \varphi_2$, where φ_1 and φ_2 denote the old φ -parameters for the two segment EME states. As will be seen below, even in the presence of the realistic noise and imperfections, an EME state is still created after a detector click. The noise only influences the success probability to get a click and the new vacuum coefficient in the EME state. In general we can express the success probability p_1 and the new vacuum coefficient c_1 as $p_1 = f_1(c_0)$ and $c_1 = f_2(c_0)$, where the functions f_1 and f_2 depend on the particular noise properties.

The above method for connecting entanglement can be cascaded to arbitrarily extend the communication distance. For the i th ($i = 1, 2, \dots, n$) entanglement connection, we first prepare in parallel two pairs of ensembles in the EME states with the same vacuum coefficient c_{i-1} and the same communication length L_{i-1} , and then perform the entanglement swapping as shown in Fig. 2, which now succeeds with a probability $p_i = f_1(c_{i-1})$. After a successful detector click, the communication length is extended to $L_i = 2L_{i-1}$, and the vacuum coefficient in the connected EME state becomes $c_i = f_2(c_{i-1})$. Since the i th entanglement connection need be repeated in average $1/p_i$ times, the total time needed to establish an EME state over the distance $L_n = 2^n L_0$ is given by

$T_n = T_0 \prod_{i=1}^n (1/p_i)$, where L_0 denotes the distance of each segment in the entanglement generation.

Entanglement-based communication schemes

After an EME state has been established between two distant sites, we would like to use it in the communication protocols, such as quantum teleportation, cryptography, and Bell inequality detection. It is not obvious that the EME state (3), which is entangled in the Fock basis, is useful for these tasks since in the Fock basis it is experimentally hard to do certain single-bit operations. In the following we will show how the EME states can be used to realize all these protocols with simple experimental configurations.

Quantum cryptography and the Bell inequality detection are achieved with the setup shown by Fig. 3a. The state of the two pairs of ensembles is expressed as $\rho_{L_1R_1} \otimes \rho_{L_2R_2}$, where $\rho_{L_iR_i}$ ($i = 1, 2$) denote the same EME state with the vacuum coefficient c_n if we have done n times entanglement connection. The φ -parameters in $\rho_{L_1R_1}$ and $\rho_{L_2R_2}$ are the same provided that the two states are established over the same stationary channels. We register only the coincidences of the two-side detectors, so the protocol is successful only if there is a click on each side. Under this condition, the vacuum components in the EME states, together with the state components $S_{L_1}^\dagger S_{L_2}^\dagger |\text{vac}\rangle$ and $S_{R_1}^\dagger S_{R_2}^\dagger |\text{vac}\rangle$, where $|\text{vac}\rangle$ denotes the ensemble state $|0_a 0_a 0_a 0_a\rangle_{L_1R_1L_2R_2}$, have no contributions to the experimental results. So, for the measurement scheme shown by Fig. 3, the ensemble state $\rho_{L_1R_1} \otimes \rho_{L_2R_2}$ is effectively equivalent to the following “polarization” maximally entangled (PME) state (the terminology of “polarization” comes from an analogy to the optical case)

$$|\Psi\rangle_{\text{PME}} = (S_{L_1}^\dagger S_{R_2}^\dagger + S_{L_2}^\dagger S_{R_1}^\dagger) / \sqrt{2} |\text{vac}\rangle. \quad (4)$$

The success probability for the projection from $\rho_{L_1R_1} \otimes \rho_{L_2R_2}$ to $|\Psi\rangle_{\text{PME}}$ (i.e., the probability to get a click on each side) is given by $p_a = 1/[2(c_n + 1)^2]$. One can also check that in Fig. 3, the phase shift ψ_Λ ($\Lambda = L$ or R) together with the corresponding beam splitter operation are equivalent to a single-bit rotation in the basis $\left\{ |0\rangle_\Lambda \equiv S_{\Lambda_1}^\dagger |0_a 0_a\rangle_{\Lambda_1\Lambda_2}, |1\rangle_\Lambda \equiv S_{\Lambda_2}^\dagger |0_a 0_a\rangle_{\Lambda_1\Lambda_2} \right\}$ with the rotation angle $\theta = \psi_\Lambda/2$. Now, it is clear how to do quantum cryptography and Bell inequality detection since we have the PME state and we can perform the desired single-bit rotations in the corresponding basis. For instance, to distribute a quantum key between the two remote sides, we simply choose ψ_Λ randomly from the set $\{0, \pi/2\}$ with an equal probability, and keep the measurement results (to be 0 if D_1^Λ clicks, and 1 if D_1^Λ clicks) on both sides as the shared secret key if the two sides become aware that they have chosen the same phase shift after the public declare. This is ex-

actly the Ekert scheme [1] and its absolute security follows directly from the proofs in [25,26]. For the Bell inequality detection, we infer the correlations $E(\psi_L, \psi_R) \equiv P_{D_1^L D_1^R} + P_{D_2^L D_2^R} - P_{D_1^L D_2^R} - P_{D_2^L D_1^R} = \cos(\psi_L - \psi_R)$ from the measurement of the coincidences $P_{D_1^L D_1^R}$ etc. For the setup shown in Fig. 3a, we would have $|E(0, \pi/4) + E(\pi/2, \pi/4) + E(\pi/2, 3\pi/4) - E(0, 3\pi/4)| = 2\sqrt{2}$, whereas for any local hidden variable theories, the CHSH inequality [27] implies that this value should be below 2.

We can also use the established long-distance EME states for faithful transfer of unknown quantum states through quantum teleportation, with the setup shown by Fig. 3b. In this setup, if two detectors click on the left side, there is a significant probability that there is no collective excitation on the right side since the product of the EME states $\rho_{L_1 R_1} \otimes \rho_{L_2 R_2}$ contains vacuum components. However, if there is a collective excitation appearing from the right side, its “polarization” state would be exactly the same as the one input from the left. So, as in the Innsbruck experiment [28], the teleportation here is probabilistic and needs posterior confirmation; but if it succeeds, the teleportation fidelity would be nearly perfect since in this case the entanglement is equivalently described by the PME state (4). The success probability for the teleportation is also given by $p_a = 1/[2(c_n + 1)^2]$, which determines the average number of repetitions for a successful teleportation.

Noise and built-in entanglement purification

We next discuss noise and imperfections in our schemes for entanglement generation, connection, and applications. In particular we show that each step contains built-in entanglement purification which makes the whole scheme resilient to the realistic noise and imperfections.

In the entanglement generation, the dominant noise is the photon loss, which includes the contributions from the channel attenuation, the spontaneous emissions in the atomic ensembles (which results in the population of the collective atomic mode with the accompanying photon going to other directions), the coupling inefficiency of the Stokes light into and out of the channel, and the inefficiency of the single-photon detectors. The loss probability is denoted by $1 - \eta_p$ with the overall efficiency $\eta_p = \eta'_p e^{-L_0/L_{\text{att}}}$, where we have separated the channel attenuation $e^{-L_0/L_{\text{att}}}$ (L_{att} is the channel attenuation length) from other noise contributions η'_p with η'_p independent of the communication distance L_0 . The photon loss decreases the success probability for getting a detector click from p_c to $\eta_p p_c$, but it has no influence on the resulting EME state. Due to this noise, the entanglement preparation time should be replaced by $T_0 \sim t_\Delta / (\eta_p p_c)$. The second source of noise comes from the dark counts of the single-photon detectors. The dark count gives a detector click, but without population of the collective atomic mode, so it contributes to the vacuum coefficient

in the EME state. If the dark count comes up with a probability p_{dc} for the time interval t_Δ , the vacuum coefficient is given by $c_0 = p_{dc} / (\eta_p p_c)$, which is typically much smaller than 1 since the Raman transition rate is much larger than the dark count rate. The final source of noise, which influences the fidelity to get the EME state, is caused by the event that more than one atom are excited to the collective mode S whereas there is only one click in D1 or D2. The conditional probability for that event is given by p_c , so we can estimate the fidelity imperfection $\Delta F_0 \equiv 1 - F_0$ for the entanglement generation by

$$\Delta F_0 \sim p_c. \quad (5)$$

Note that by decreasing the excitation probability p_c , one can make the fidelity imperfection closer and closer to zero with the price of a longer entanglement preparation time T_0 . This is the basic idea of the entanglement purification. So, in this scheme, the confirmation of the click from the single-photon detector generates and purifies entanglement at the same time.

In the entanglement swapping, the dominant noise is still the losses, which include the contributions from the detector inefficiency, the inefficiency of the excitation transfer from the collective atomic mode to the optical mode [20,21], and the small decay of the atomic excitation during the storage [19–21]. Note that by introducing the detector inefficiency, we have automatically taken into account the imperfection that the detectors cannot distinguish the single and the two photons. With all these losses, the overall efficiency in the entanglement swapping is denoted by η_s . The loss in the entanglement swapping gives contributions to the vacuum coefficient in the connected EME state, since in the presence of loss a single detector click might result from two collective excitations in the ensembles I_1 and I_2 , and in this case, the collective modes in the ensembles L and R have to be in a vacuum state. After taking into account the realistic noise, we can specify the success probability and the new vacuum coefficient for the i th entanglement connection by the recursion relations $p_i \equiv f_1(c_{i-1}) = \eta_s \left(1 - \frac{\eta_s}{2(c_{i-1}+1)}\right) / (c_{i-1}+1)$ and $c_i \equiv f_2(c_{i-1}) = 2c_{i-1} + 1 - \eta_s$. The coefficient c_0 for the entanglement preparation is typically much smaller than $1 - \eta_s$, then we have $c_i \approx (2^i - 1)(1 - \eta_s) = (L_i/L_0 - 1)(1 - \eta_s)$, where L_i denotes the communication distance after i times entanglement connection. With the expression for the c_i , we can easily evaluate the probability p_i and the communication time T_n for establishing a EME state over the distance $L_n = 2^n L_0$. After the entanglement connection, the fidelity of the EME state also decreases, and after n times connection, the overall fidelity imperfection $\Delta F_n \sim 2^n \Delta F_0 \sim (L_n/L_0) \Delta F_0$. We need fix ΔF_n to be small by decreasing the excitation probability p_c in Eq. (5).

It is important to point out that our entanglement connection scheme also has built-in entanglement purification function. This can be understood as follows: Each time we connect entanglement, the imperfections of the setup decrease the entanglement fraction $1/(c_i + 1)$ in the EME state. However, the entanglement fraction decays only linearly with the distance (the number of segments), which is in contrast to the exponential decay of the entanglement for the connection schemes without entanglement purification. The reason for the slow decay is that in each time of the entanglement connection, we need repeat the protocol until there is a detector click, and the confirmation of a click removes part of the added vacuum noise since a larger vacuum components in the EME state results in more times of repetitions. The built-in entanglement purification in the connection scheme is essential for the polynomial scaling law of the communication efficiency.

As in the entanglement generation and connection schemes, our entanglement application schemes also have built-in entanglement purification which makes them resilient to the realistic noise. Firstly, we have seen that the vacuum components in the EME states are removed from the confirmation of the detector clicks and thus have no influence on the fidelity of all the application schemes. Secondly, if the single-photon detectors and the atom-to-light excitation transitions in the application schemes are imperfect with the overall efficiency denoted by η_a , one can easily check that these imperfections only influence the efficiency to get the detector clicks with the success probability replaced by $p_a = \eta_a / [2(c_n + 1)^2]$, and have no effects on the communication fidelity. Finally, we have seen that the phase shifts in the stationary channels and the small asymmetry of the stationary setup are removed automatically when we project the EME state to the PME state, and thus have no influence on the communication fidelity.

The noise not correctable by our scheme includes the detector dark count in the entanglement connection and the non-stationary channel noise and set asymmetries. The resulting fidelity imperfection from the dark count increases linearly with the number of segments L_n/L_0 , and from the non-stationary channel noise and set asymmetries increases by the random-walk law $\sqrt{L_n/L_0}$. For each time of entanglement connection, the dark count probability is about 10^{-5} if we make a typical choice that the collective emission rate is about 10MHz and the dark count rate is 10^2 Hz. So this noise is negligible even if we have communicated over a long distance (10^3 the channel attenuation length L_{att} for instance). The non-stationary channel noise and setup asymmetries can also be safely neglected for such a distance. For instance, it is relatively easy to control the non-stationary asymmetries in local laser operations to values below 10^{-4} with the use of accurate polarization techniques [29] for Zee-

man sublevels (as in Fig. 2b).

Scaling of the communication efficiency

We have shown that each of our entanglement generation, connection, and application schemes has built-in entanglement purification, and as a result of this property, we can fix the communication fidelity to be nearly perfect, and at the same time keep the communication time to increase only polynomially with the distance. Assume that we want to communicate over a distance $L = L_n = 2^n L_0$. By fixing the overall fidelity imperfection to be a desired small value ΔF_n , the entanglement preparation time becomes $T_0 \sim t_\Delta / (\eta_p \Delta F_0) \sim (L_n/L_0) t_\Delta / (\eta_p \Delta F_n)$. For an effective generation of the PME state (4), the total communication time $T_{\text{tot}} \sim T_n/p_a$ with $T_n \sim T_0 \prod_{i=1}^n (1/p_i)$. So the total communication time scales with the distance by the law

$$T_{\text{tot}} \sim 2(L/L_0)^2 / (\eta_p p_a \Delta F_T \prod_{i=1}^n p_i), \quad (6)$$

where the success probabilities p_i, p_a for the i th entanglement connection and for the entanglement application have been specified before. The expression (6) has confirmed that the communication time T_{tot} increases with the distance L only polynomially. We show this explicitly by taking two limiting cases. In the first case, the inefficiency $1 - \eta_s$ for the entanglement swapping is assumed to be negligibly small. One can deduce from Eq. (6) that in this case the communication time $T_{\text{tot}} \sim T_{\text{con}} (L/L_0)^2 e^{L_0/L_{\text{att}}}$, with the constant $T_{\text{con}} \equiv 2t_\Delta / (\eta_p' \eta_a \Delta F_T)$ being independent of the segment and the total distances L_0 and L . The communication time T_{tot} increases with L quadratically. In the second case, we assume that the inefficiency $1 - \eta_s$ is considerably large. The communication time in this case is approximated by $T_{\text{tot}} \sim T_{\text{con}} (L/L_0)^{[\log_2(L/L_0)+1]/2+\log_2(1/\eta_s-1)+2} e^{L_0/L_{\text{att}}}$, which increases with L still polynomially (or sub-exponentially in a more accurate language, but this makes no difference in practice since the factor $\log_2(L/L_0)$ is well bounded from above for any reasonably long distance). If T_{tot} increases with L/L_0 by the m th power law $(L/L_0)^m$, there is an optimal choice of the segment length to be $L_0 = mL_{\text{att}}$ to minimize the time T_{tot} . As a simple estimation of the improvement in the communication efficiency, we assume that the total distance L is about $100L_{\text{att}}$, for a choice of the parameter $\eta_s \approx 2/3$, the communication time $T_{\text{tot}}/T_{\text{con}} \sim 10^6$ with the optimal segment length $L_0 \sim 5.7L_{\text{att}}$. This result is a dramatic improvement compared with the direct communication case, where the communication time T_{tot} for getting a PME state increases with the distance L by the exponential law $T_{\text{tot}} \sim T_{\text{con}} e^{L/L_{\text{att}}}$. For the same distance $L \sim 100L_{\text{att}}$, one needs $T_{\text{tot}}/T_{\text{con}} \sim 10^{43}$ for direct communication, which means that for this example the present scheme is 10^{37} times more efficient.

Outlook

We have presented a novel approach for implementation of quantum repeaters and long-distance quantum communication. The proposed technique allows to generate and connect the entanglement and use it in quantum teleportation, cryptography, and tests of Bell inequalities. All of the elements of the present scheme are within the reach of current experimental technology, and all have the important property of built-in entanglement purification which makes them resilient to the realistic noise. As a result, the overhead required to implement the present scheme, such as the communication time, scales polynomially with the channel length. This is in dramatic contrast to direct communication where the exponential overhead is required. Such an efficient scaling, combined with a relative simplicity of the experimental setup, opens up realistic prospective for quantum communication over long distances.

-
- [1] Ekert, A. Quantum cryptography based on Bell's theorem. *Phys. Rev. Lett.* **67**, 661-663 (1991).
 - [2] Bennett, C. H. *et al.* Teleporting an unknown quantum state via dual classical and Einstein-Podolsky-Rosen channels. *Phys. Rev. Lett.* **73**, 3081-3084 (1993).
 - [3] Bennett, C. H. *et al.* Purification of noisy entanglement and faithful teleportation via noisy channels. *Phys. Rev. Lett.* **76**, 722-725 (1991).
 - [4] Briegel, H.-J., Duer, W., Cirac, J. I. & Zoller, P. Quantum repeaters: The role of imperfect local operations in quantum communication. *Phys. Rev. Lett.* **81**, 5932-5935 (1991).
 - [5] Knill, E., Laflamme, R. & Zurek, W. H. Resilient quantum computation. *Science* **279**, 342-345 (1998).
 - [6] Preskill, J. Reliable quantum computers. *Proc. R. Soc. Lond. A* **454**, 385-410 (1998).
 - [7] Zukowski, M., Zeilinger, A., Horne, M. A. & Ekert, A. "Event-ready-detectors" Bell experiment via entanglement swapping. *Phys. Rev. Lett.* **71**, 4287 (1993).
 - [8] Cirac, J. I., Zoller, P., Kimble, H. J. & Mabuchi, H. Quantum state transfer and entanglement distribution among distant nodes in a quantum network, *Phys. Rev. Lett.* **78**, 3221-3224 (1997).
 - [9] Enk, S. J., Cirac, J. I. & Zoller, P. Photonic channels for quantum communication, *Science* **279**, 205-207 (1998).
 - [10] Ye, J., Vernooy, D. W. & Kimble, H. J. Trapping of single Atoms in cavity QED. *Phys. Rev. Lett.* **83**, 4987-4990 (1999).
 - [11] Hood, C. J. *et al.* The atom-cavity microscope: Single atoms bound in orbit by single photons, *Science* **287**, 1447-1453 (2000).
 - [12] Pinkse, P. W. H. Fischer, T. Maunz, T. P. & Rempe, G. Trapping an atom with single photons. *Nature* **404**, 365 - 368 (2000).
 - [13] Cibrillo, C. Cirac, J. I., G-Fernandez, P. & Zoller, P. Creation of entangled states of distant atoms by interference. *Phys. Rev. A* **59**, 1025-1033 (1999).
 - [14] Bose, S., Knight, P. L., Plenio, M. B. & Vedral, V. Proposal for Teleportation of an Atomic State via Cavity Decay, *Phys. Rev. Lett.* **83**, 5158-5161 (1999).
 - [15] Mostowski, J. & Sobolewska, B. Transverse effects in stimulated Raman scattering. *Phys. Rev. A* **30**, 610-612 (1984).
 - [16] Kuzmich A., Bigelow, N. P. & Mandel, L. Atomic quantum non-demolition measurements and squeezing. *Europhys. Lett. A* **42**, 481 (1998).
 - [17] Fleischhauer, M. & Lukin, M. D. Dark-state polaritons in electromagnetically induced transparency. *Phys. Rev. Lett.* **84**, 5094-5097 (2000).
 - [18] Duan, L. M., Cirac, J. I., Zoller, P. & Polzik, E. S. Quantum communication between atomic ensembles using coherent light, *Phys. Rev. Lett.* **85**, 5643-5646 (2000).
 - [19] Hald, J., Sorensen, J. L., Schori, C. & Polzik, E. S. Spin squeezed state: A macroscopic entangled ensemble created by light. *Phys. Rev. Lett.* **83**, 1319-1322 (1999).
 - [20] Phillips, D. F. *et al.* Storage of light in atomic vapor. *Phys. Rev. Lett.* **86**, 783-786 (2001).
 - [21] Liu, C., Dutton, Z., Behroozi, C. H. & Hau, L. V. Observation of coherent optical information storage in an atomic medium using halted light pulses. *Nature* **409**, 490-493 (2001).
 - [22] Knill, E., Laflamme, R. & Milburn G. J. A scheme for efficient quantum computation with linear optics. *Nature* **409**, 46-52 (2001).
 - [23] Pan, J. W., Simon, C., Brukner, C. & Zeilinger, A. Feasible entanglement purification for quantum communication. *Nature* **410**, 1067-1070 (2001).
 - [24] Roch, J.-F. *et al.* Quantum Nondemolition Measurements using Cold Trapped Atoms. *Phys. Rev. Lett.* **78**, 634-637 (1997).
 - [25] Lo, H. K. & Chau, H. F. *Science* **283**, 2050-2056 (1999).
 - [26] Shor, P. W. & Preskill, J. Simple proof of security of the BB84 quantum key distribution protocol. *Phys. Rev. Lett.* **85**, 441-444 (2000).
 - [27] Clauser, J. F. Horne, M. A. Shimony, A. & Holt, R. A. *Phys. Rev. Lett.* **23**, 880 (1969).
 - [28] Bouwmeester, D. *et al.* Experimental quantum teleportation. *Nature* **390**, 575-579 (1997).
 - [29] Budker, D., Yashuk V., and Zolotarev, M. Nonlinear magneto-optic effects with ultranarrow width. *Phys. Rev. Lett.* **81**, 5788-5791 (1998).

Acknowledgments This work was supported by the Austrian Science Foundation, the Europe Union project EQUIP, the ESF, the European TMR network Quantum Information, and the NSF through the grant to the ITAMP. L.M.D. thanks in addition the support from the Chinese Science Foundation.

Box 1: Collective enhancement

Long-lived excitations in atomic ensemble can be viewed as waves of excited spins. We are here particularly interested in symmetric spin wave mode S . For a simple demonstration of the collective enhancement, we assume that atoms are placed in a low finesse ring cavity [24], with a relevant cavity mode corresponding to forward-scattered Stokes radiation. Cavity-free case corresponds to the limit where the finesse tends to 1 [16]. The interaction between the forward-scattered light mode and atoms is described by the Hamiltonian

$$H = \hbar \left(\sqrt{N_a} \Omega g_c / \Delta \right) S^\dagger b^\dagger + \text{h.c.},$$

where b^\dagger is creation operator for cavity photon, Ω is the laser Rabi frequency, and g_c atom-field coupling constant. In addition to coherent evolution the photonic field mode can leak out of the cavity at a rate κ , whereas atomic coherence is dephased by spontaneous photon scattering into random directions that occurs at a rate $\gamma'_s = \Omega^2 / \Delta^2 \gamma_s$ for each atom, with γ_s being the natural linewidth of the electronic excited state. We emphasize that in the absence of superradiant effects spontaneous emission events are independent for each atom.

In the bad-cavity limit, we can adiabatically eliminate the cavity mode, and the resulting dynamics for the collective atomic mode is described by the Heisenberg-Langevin equation (see the supplementary information for details)

$$\dot{S}^\dagger = \frac{(\kappa' - \gamma'_s)}{2} S^\dagger - \sqrt{\kappa'} b_{in}(t) + \text{noise},$$

where $\kappa' = 4|\Omega|^2 g_c^2 N_a / (\Delta^2 \kappa)$, b_{in} is a vacuum field leaking into the cavity, and the last term represents the fluctuating noise field corresponding to the spontaneous emission. Note that nature of the dynamics is determined by ratio between the build-up of coherence due to forward-scattered photons κ' and coherence decay due to spontaneous emission γ'_s . The signal-to-noise ratio is therefore given by $R = \kappa' / \gamma_s \equiv 4N_a g_c^2 / (\kappa \gamma)$, which is large when many-atom ensemble is used. In the cavity-free case this expression corresponds to optical depth (density-length product) of the sample. The result should be compared with the signal-to-noise ratio in the single-atom case $N_a = 1$, where to obtain $R > 1$ a high-Q microcavity is required [10–12]. The collective enhancement takes place since the coherent forward scattering involves only one collective atomic mode S , whereas the spontaneous emissions distribute excitation over all atomic modes. Therefore only a small fraction of spontaneous emission events influences the symmetric mode S , which results in a large signal-to-noise ratio.

Caption for Fig. 1 (1a) The relevant level structure of the atoms in the ensemble with $|g\rangle$, the ground state, $|s\rangle$, the metastable state for storing a qubit, and $|e\rangle$, the excited state. The transition $|g\rangle \rightarrow |e\rangle$ is coupled by the classical laser with the Rabi frequency Ω , and the forward scattering Stokes light comes from the transition $|e\rangle \rightarrow |s\rangle$. For convenience, we assume off-resonant coupling with a large detuning Δ . (1b) Schematic setup for generating entanglement between the two atomic ensembles L and R. The two ensembles are pencil shaped and illuminated by the synchronized classical laser pulses. The forward-scattering Stokes pulses are collected after the filters (polarization and frequency selective) and interfered at a 50%-50% beam splitter BS after the transmission channels, with the outputs detected respectively by two single-photon detectors D1 and D2. If there is a click in D1 or D2, the process is finished and we successfully generate entanglement between the ensembles L and R. Otherwise, we first apply a repumping pulse to the transition $|s\rangle \rightarrow |e\rangle$ on the ensembles L and R to set the state of the ensembles back to the ground state $|0\rangle_a^L \otimes |0\rangle_a^R$, then the same classical laser pulses as the first round are applied to the transition $|g\rangle \rightarrow |e\rangle$ and we detect again the forward-scattering Stokes pulses after the beam splitter. This process is repeated until finally we have a click in the D1 or D2 detector.

Caption for Fig. 2. (2a) Illustrative setup for the entanglement swapping. We have two pairs of ensembles L, I_1 and I_2 , R distributed at three sites L, I and R. Each of the ensemble-pairs L, I_1 and I_2 , R is prepared in an EME state in the form of Eq. (3). The excitations in the collective modes of the ensembles I_1 and I_2 are transferred simultaneously to the optical excitations by the repumping pulses applied to the atomic transition $|s\rangle \rightarrow |e\rangle$, and the stimulated optical excitations, after a 50%-50% beam splitter, are detected by the single-photon detectors D1 and D2. If either D1 or D2 clicks, the protocol is successful and an EME state in the form of Eq. (3) is established between the ensembles L and R with a doubled communication distance. Otherwise, the process fails, and we need to repeat the previous entanglement generation and swapping until finally we have a click in D1 or D2, that is, until the protocol finally succeeds. (2b) The two intermediated ensembles I_1 and I_2 can also be replaced by one ensemble but with two metastable states I_1 and I_2 to store the two different collective modes. The 50%-50% beam splitter operation can be simply realized by a $\pi/2$ pulse on the two metastable states before the collective atomic excitations are transferred to the optical excitations.

Caption for Fig. 3 (3a) Schematic setup for the realization of quantum cryptography and Bell inequality detection. Two pairs of ensembles L_1, R_1 and L_2, R_2 (or two pairs of metastable states as shown by Fig. (2b)) have been prepared in the EME states. The collective atomic excitations on each side are transferred to

the optical excitations, which, respectively after a relative phase shift φ_L or φ_R and a 50%-50% beam splitter, are detected by the single-photon detectors D_1^L, D_2^L and D_1^R, D_2^R . We look at the four possible coincidences of D_1^R, D_2^R with D_1^L, D_2^L , which are functions of the phase difference $\varphi_L - \varphi_R$. Depending on the choice of φ_L and φ_R , this setup can realize both the quantum cryptography and the Bell inequality detection. (3b) Schematic setup for probabilistic quantum teleportation of the atomic “polarization” state. Similarly, two pairs of ensembles L_1, R_1 and L_2, R_2 are prepared in the EME states. We want to teleport an atomic “polarization” state $(d_0 S_{I_1}^\dagger + d_1 S_{I_2}^\dagger) |0_a 0_a\rangle_{I_1 I_2}$ with unknown coefficients d_0, d_1 from the left to the right side, where $S_{I_1}^\dagger, S_{I_2}^\dagger$ denote the collective atomic operators for the two ensembles I_1 and I_2 (or two metastable states in the same ensemble). The collective atomic excitations in the ensembles I_1, L_1 and I_2, L_2 are transferred to the optical excitations, which, after a 50%-50% beam splitter, are detected by the single-photon detectors D_1^I, D_1^L and D_2^I, D_2^L . If there are a click in D_1^I or D_1^L and a click in D_2^I or D_2^L , the protocol is successful. A π -phase rotation is then performed on the collective mode of the ensemble R_2 conditional on that the two clicks appear in the detectors D_1^I, D_2^L or D_2^I, D_1^L . The collective excitation in the ensembles R_1 and R_2 , if appearing, would be found in the same “polarization” state $(d_0 S_{R_1}^\dagger + d_1 S_{R_2}^\dagger) |0_a 0_a\rangle_{R_1 R_2}$.

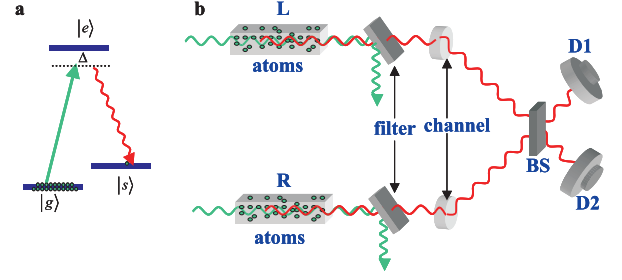


FIG. 1.

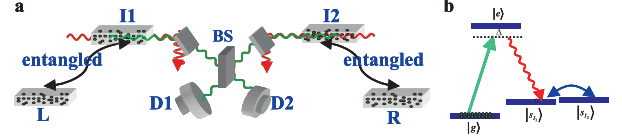


FIG. 2.

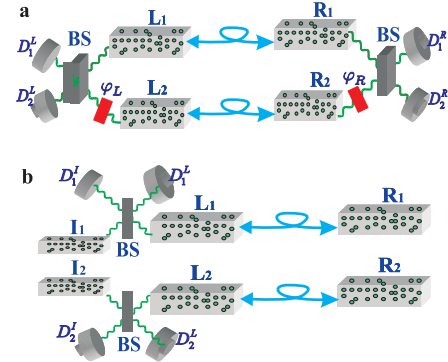


FIG. 3.

Long-distance quantum communication with atomic ensembles and linear optics: Supplementary information

L.-M. Duan^{1,2*}, M. Lukin³, J. I. Cirac^{1†}, and P. Zoller¹

¹*Institut für Theoretische Physik, Universität Innsbruck, A-6020 Innsbruck, Austria*

²*Laboratory of Quantum Communication and Computation, USTC, Hefei 230026, China*

³*ITAMP, Harvard-Smithsonian Center for Astrophysics, Cambridge, MA 02138*

I. LIGHT-ATOM INTERACTION AND THE COLLECTIVE ENHANCEMENT OF THE SIGNAL-TO-NOISE RATIO

We demonstrate in the following that when optical pulses interact with an sample of atoms with the Λ level configuration, there is a collective enhancement of the signal-to-noise ratio for the collective atomic mode. For a simple demonstration of the collective effects, we first assume there is a (low finesse) ring cavity around the ensemble as shown by Fig. 1. The case of the free-space ensemble corresponds the limit that the cavity finesse tends to 1 [1]. A classical laser with the wave vector $k_l = \omega_l/c$ is coupling to the transition $|g\rangle \rightarrow |e\rangle$ with a Rabi frequency Ω , and the ring cavity mode b with the wave vector $k_s = \omega_s/c$ is coupling to the transition $|e\rangle \rightarrow |s\rangle$ and with a coupling coefficient g_c . For simplicity, first we assume off-resonant coupling with a large detuning Δ as shown by Fig. S1. The classical laser is co-propagating with the ring cavity mode to satisfy the collective condition $(k_l - k_s)L_a \ll \pi$, where L_a is the length of the pencil-shape atomic ensemble. With this condition, after we adiabatically eliminate the upper level $|e\rangle$, the Hamiltonian has the following form in the rotating frame

$$H = \hbar \left(\sqrt{N_a} \Omega g_c / \Delta \right) S^\dagger b^\dagger + \text{h.c.}, \quad (1)$$

where S is the collective atomic mode defined in the text which has the form $S \equiv (1/\sqrt{N_a}) \sum_i S_i$ with $S_i = |g\rangle_i \langle s|$, the individual atomic lowering operator. There should be also some light shift terms, but they can be trivially canceled by refining the laser frequency. Corresponding to the Hamiltonian (1), the Heisenberg-Langevin equations for the modes S and b are respectively given by [2]

$$\dot{b} = -i \left(\sqrt{N_a} \Omega g_c / \Delta \right) S^\dagger - (\kappa/2) b - \sqrt{\kappa} b_{in}(t), \quad (2)$$

$$\dot{S}^\dagger = i \left(\sqrt{N_a} \Omega^* g_c^* / \Delta \right) b, \quad (3)$$

where κ is the cavity decay rate, and $b_{in}(t)$ is the input vacuum field with the properties $[b_{in}(t), b_{in}^\dagger(t')] =$

$\delta(t-t')$ and $\langle b_{in}^\dagger(t) b_{in}(t) \rangle = 0$. The output field $b_{out}(t)$ from the cavity (the Stokes light) is connected with the input by the input-output relation $b_{out}(t) = b_{in}(t) + \sqrt{\kappa} b(t)$. In obtaining Eq. (3), we have used the weak interaction condition which assumes after the interaction most of the atoms are still in the ground state so that $[S, S^\dagger] = \sum_i (|g\rangle_i \langle g| - |s\rangle_i \langle s|) / N_a \simeq 1$. We have not included in Eq. (3) the atomic spontaneous emission, which will introduce some heating effects to the mode S and will be discussed later. In the bad-cavity limit $\kappa \gg \sqrt{N_a} |\Omega g_c| / \Delta$, we can adiabatically eliminate the cavity mode b , and the resulting equation is

$$\dot{S}^\dagger = \frac{\kappa'}{2} S^\dagger - \sqrt{\kappa'} b_{in}(t), \quad (4)$$

where the effective interaction coefficient $\kappa' = 4N_a |\Omega g_c|^2 / (\Delta^2 \kappa)$, and without loss of generality we assumed the phase of the laser is chosen in the way $i\Omega^* g_c^* = |\Omega g_c|$. The output optical field, expressed by the operator S^\dagger , has the form $b_{out}(t) = -b_{in}(t) + \sqrt{\kappa'} S^\dagger(t)$. Equation (4) is linear and has the explicit solution

$$S^\dagger(t) = S^\dagger(0) e^{\kappa' t/2} - \sqrt{\kappa'} \int_0^t e^{\kappa'(t-\tau)/2} b_{in}(\tau) d\tau, \quad (5)$$

From this, we easily get the solution for the output optical field $b_{out}(t)$.

What we measure (without beam splitters) by the photon detector is the integration of the photon current for the detection time interval t_Δ , which is proportional to the intensity integration of the output field. So we measure the operator $Q_m = \int_0^{t_\Delta} b_{out}^\dagger(\tau) b_{out}(\tau) d\tau$. One can find an explicit expression for Q_m by substituting the solution of $b_{out}(t)$. To simplify it, we define an effective single-mode bosonic operator a from the continuous field $b_{in}(t)$ with the form

$$a \equiv -\frac{\sqrt{\kappa'}}{\sqrt{e^{\kappa' t_\Delta} - 1}} \int_0^{t_\Delta} e^{\kappa'(t_\Delta - \tau)/2} b_{in}(\tau) d\tau. \quad (6)$$

With this operator, the measured quantity is expressed as

$$Q_m = a_t^\dagger a_t + \int_0^{t_\Delta} b_{in}^\dagger(\tau) b_{in}(\tau) d\tau, \quad (7)$$

where $a_{t_\Delta} = a \cosh r_c + S^\dagger(0) \sinh r_c$, a Bogoliubov transformation of a and $S^\dagger(0)$ with $\cosh r_c \equiv e^{\kappa' t_\Delta/2}$. The

*Email: luming.duan@uibk.ac.at

†Email: Ignacio.Cirac@uibk.ac.at

last term of Eq. (7) is a trivial integration of the intensity of the vacuum field, which has no contribution to the measurement result. So what we measure is in fact the photon number in the defined effective mode. Note that Eq. (5) can also be written in the Bogoliubov form $S^\dagger(t_\Delta) = S^\dagger(0) \cosh r_c + a \sinh r_c$ with $S^\dagger(0)$ and a respectively in the atomic and photonic vacuum states $|0_a\rangle$ and $|0_p\rangle$. Transferring to the Schrodinger picture, we conclude that after time t_Δ the collective atomic mode and the effective mode for the Stokes light are in a two-mode squeezed state

$$|\phi\rangle = \sec r_c \sum_n (S^\dagger a \tanh r_c)^n |0_a\rangle |0_p\rangle. \quad (8)$$

This is exactly the state (1) in the paper if the excitation probability $p_c = \tanh^2 r_c \ll 1$, and we have shown above that the detector measures the photon number in the effective mode a . If there are two ensembles and the detectors are put after a beam splitter as discussed in the paper, it is straightforward to extend the above treatment to see that one measures the photon numbers in the effective modes a_\pm (see in the paper for the definitions). So we confirm the results there.

Now let us take into account the atomic spontaneous emissions from the level $|e\rangle$ to $|s\rangle$. The photons from spontaneous emissions go to the free-space modes (other than the cavity mode b) with random directions, and we assume that the atomic ensemble is dilute with $k_s/\sqrt[3]{\rho_n} \gg 1$ (where ρ_n is the atomic number density) so that there is no superradiance. Each atom undergoes spontaneous emissions independently with the rate $\gamma'_s = (\Omega^2/\Delta^2)\gamma_s$, where γ_s denotes the on-resonance spontaneous emission rate. The spontaneous emission introduces a coherence decay term to the Langevin equation of the individual atomic operator S_i

$$\dot{S}_i^\dagger = -(\gamma'_s/2) S_i^\dagger + \text{noise}, \quad (9)$$

where the last term represents the corresponding fluctuation from the noise field which results in heating, and we have left out in Eq. (9) the coherent interaction term from the Hamiltonian. By taking summation of Eq. (9) over all the atoms, we immediately see that there is added coherence decay term to the Langevin equation (4) of the collective atomic operator S^\dagger with the decay rate still given by γ'_s . The ratio R_{sn} between the coherent interaction rate κ' and the decay rate γ'_s (called the signal-to-noise ratio in the following) is given by $R_{sn} = 4N_a |g_c|^2 / (\kappa\gamma_s)$. In the single-atom case, the signal-to-noise ratio is about $4|g_c|^2 / (\kappa\gamma_s)$. So, for the atomic ensemble, the signal-to-noise ratio, which influences the collection efficiency in our scheme (see the paper for the discussions on noise), is greatly enhanced by the large factor of the atom number. This enhancement comes from the fact that the coherent interaction producing the co-propagating signal involves only the collective

atomic mode S , whereas the independent spontaneous emissions distribute over all the atomic modes, and thus only have small influence on the interesting mode S . As a result of the collective enhancement, a weak-coupling cavity has assured a large signal-to-noise ratio for the interesting mode.

The collective enhancement of the signal-to-noise ratio can also be easily understood if one looks at the master equation. The whole density operator ρ_w for the atomic internal states and the cavity mode obeys the following master equation [2]

$$\dot{\rho}_w = i[\rho_w, H] + \kappa \hat{L}[b] \rho_w + \gamma'_s \sum_i \hat{L}[S_i^\dagger] \rho_w, \quad (10)$$

where the Liouville superoperators $\hat{L}[X]$ ($X = b, S_i^\dagger$) are defined as $\hat{L}[X] \rho_w \equiv X \rho_w X^\dagger - (X^\dagger X \rho_w + \rho_w X^\dagger X)/2$. In Eq. (10), the first term of the right hand side (r.h.s.) comes from the Hamiltonian interaction, the second term represents the cavity output coupling, and the last term describes independent spontaneous emissions for individual atomic operators. In the bad cavity limit, after adiabatically eliminating the cavity mode, we get from Eqs. (10) and (1) the following master equation for the traced atomic density operator ρ_a

$$\dot{\rho}_a = \kappa' \hat{L}[S^\dagger] \rho_a + \gamma'_s \sum_i \hat{L}[S_i^\dagger] \rho_a, \quad (11)$$

where $\hat{L}[S^\dagger]$ is the Liouville superoperator for the collective atomic mode. The above equation can be further simplified if we introduce the Fourier transformation to the individual atomic operators S_j ($j = 0, 1, \dots, N_a - 1$) with the form $S_\mu \equiv \sum_j S_j e^{ij\mu/N_a} / \sqrt{N_a}$, where $S_{\mu=0}$ gives exactly the collective atomic operator S . In terms of the operators S_μ , the master equation has the form

$$\dot{\rho}_a = (\kappa' + \gamma'_s) \hat{L}[S^\dagger] \rho_a + \gamma'_s \sum_{\mu \neq 0} \hat{L}[S_\mu^\dagger] \rho_a, \quad (12)$$

Under the weak interaction condition $\langle S_j^\dagger S_j \rangle \ll 1$, the operators S_μ ($\mu = 0, 1, \dots, N_a - 1$) commute with each other, so they represent independent atomic modes. We are only interested in the collective atomic mode S , and the populations in all the other modes S_μ with $\mu \neq 0$ have no influence on the state and the measurement of the mode S . (To measure the state of the mode S , we transfer the collective atomic excitation to the optical excitation as described in the paper. The details on the excitation transferring can be found in Refs. [3,4]). So we can trace over the modes S_μ ($\mu \neq 0$) and eliminate the last term in Eq. (12). There are two contributions to the population in the collective atomic mode: the one with a rate κ' produces a coherent output signal, and the one with a rate γ'_s emits photons to other random directions. The signal-to-noise ratio is again given by

$R_{sn} = \kappa'/\gamma'_s \sim 4N_a |g_c|^2 / (\kappa\gamma_s)$. It is interesting to note from Eq. (12) that the total spontaneous emission rate of all the modes is $N_a\gamma'_s$, which could be much larger than the coherent interaction rate κ' , however, the spontaneous emission rate for the collective atomic mode is N_a times smaller than the total rate, and the spontaneous emissions going to other modes have no influence on the scheme. So we have a large signal-to-noise ratio. The collective enhancement of the signal-to-noise ratio has been used in several schemes [1,3-5] and has been demonstrated by the recent experiments [6-8].

In our scheme by no means we necessarily need a good cavity, since on the one hand the signal-to-noise ratio in our scheme influences only the efficiency instead of the fidelity, and on the other hand, due to the collective enhancement shown above, we could still have a considerably large signal-to-noise ratio even without a cavity. In fact, we can assume to continuously decrease the cavity finesse down to 1, i.e., to the free-space limit. In the free-space limit, the cavity decay rate κ is estimated by c/L_a , the inverse of the traveling time of the pulse in the ensemble. With the well known expressions for the coefficients g_c and γ_s [5], one can estimate the signal-to-noise ratio in the free-space limit by $R_{sn} \sim 4N_a |g_c|^2 / (\kappa\gamma_s) \sim 3\rho_n L_a / k_s^2 \sim d_o$, where d_o denotes the on-resonance optical depth of the atomic ensemble which can be quite large with the current experimental technology [6-8]. So we can have a considerably large signal-to-noise ratio for the collective atomic mode even in the free-space case. A detailed treatment of the free-space light-atom interaction can be found in Refs. [9,10].

atomic medium using halted light pulses. *Nature* **409**, 490-493 (2001).

- [8] Kuzmich, A., Mandel, L. & Bigelow, N. P. Generation of spin squeezing via continuous quantum non-demolition measurement. *Phys. Rev. Lett.* **85**, 1594-1597 (2000).
- [9] Raymer, M. G. & Mostowski, J. *Phys. Rev. A* **24**, 1980 (1981).
- [10] Mostowski, J. & Sobolewska, B. Transverse effects in stimulated Raman scattering. *Phys. Rev. A* **30**, 610-612 (1984).

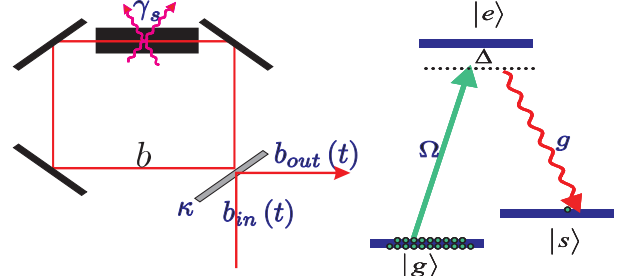


FIG. 1. Schematic system configuration

-
- [1] Kuzmich A., Bigelow, N. P. & Mandel, L. Atomic quantum non-demolition measurements and squeezing. *Europhys. Lett. A* **42**, 481 (1998).
 - [2] Gardiner, C. W. & Zoller, P. *Quantum Noise* (Springer-Verlag, Berlin, 1999).
 - [3] Lukin, M. D., Yelin, S. F. & Fleischhauer, M. Entanglement of atomic ensembles by trapping correlated photon states *Phys. Rev. Lett.* **84**, 4232-4235 (2000). Duan, L. M., Cirac, J. I., Zoller, P. (unpublished).
 - [4] Fleischhauer, M. & Lukin, M. D. Dark-state polaritons in electromagnetically induced transparency. *Phys. Rev. Lett.* **84**, 5094-5097 (2000).
 - [5] Duan, L. M., Cirac, J. I., Zoller, P. & Polzik, E. S. Quantum communication between atomic ensembles using coherent light, *Phys. Rev. Lett.* **85**, 5643-5646 (2000);
 - [6] Phillips, D. F. *et al.* Storage of light in atomic vapor. *Phys. Rev. Lett.* **86**, 783-786 (2001).
 - [7] Liu, C., Dutton, Z., Behroozi, C. H. & Hau, L. V. Observation of coherent optical information storage in an